Proceedings of 2004 IEEE/RSJ International Conference on
Intelligent Robots and Systems
September 28 - October 2, 2004, Sendai, Japan

Sensor-based machine olfaction with a neurodynamics model of the olfactory bulb

B. Raman, A. Gutierrez-Galvez, A. Perera-Lluna and R. Gutierrez-Osuna*
Department of Computer Science
Texas A&M University
College Station, TX, USA
{barani, agustin, aperera, rgutier}@cs.tamu.edu

Abstract— **We propose a biologically inspired model of olfactory processing for chemosensor arrays. The model captures three functions in the early olfactory pathway: chemotopic convergence of receptor neurons onto the olfactory bulb, center on-off surround lateral interactions, and adaptation to sustained stimuli. The projection of ORNs onto glomerular units is simulated with a self-organizing model of chemotopic convergence, which leads to odor-specific spatial patterning. This information serves as an input to a network of mitral cells with center on-off surround lateral inhibition, which enhances the initial contrast among odors and decouples odor identity from intensity. Finally, slow adaptation of mitral cells adds a temporal dimension to the spatial patterns that further enhances odor discrimination. The model is validated using experimental data from an array of temperature-modulated metal-oxide sensors.**

Keywords--: Machine olfaction, neurodynamics, olfactory coding, self-organization, lateral inhibition, sensory adaptation.

I. INTRODUCTION

Olfaction is a primary sense for most animal species. Olfactory cues are extensively used for food foraging, trail following, mating, bonding, navigation, and detection of threats. Compared to other sensing modalities, however, the use of olfaction in mobile robotics is still in its early stages. From a signal processing perspective, the use of machine olfaction as primary robotic sense poses a number of challenges, including sensor drift compensation, concentration-invariant recognition, orthogonalization of odor patterns, mixture separation, and identification against interferents and/or complex odor backgrounds.

Our research focuses on computational models of olfactory processing in the context of machine olfaction with chemosensor arrays. Following a growing movement in neuromorphic systems research [1], which argues in favor of the use of robots as physical models to test hypotheses of animal behavior, we believe that chemosensor arrays provide an opportunity to test plausible models of olfactory processing and, by extension, of olfaction-driven animal behaviors.

To this end, Marques et al. [2] have compared several biologically-inspired chemotaxic behaviors for odor source localization with mobile robots. Grasso et al. [3] have developed a biomimetic robot lobster capable of tracking chemical plumes underwater. Hayes et al. [4] have investigated distributed approaches for odor source localization with teams of mobile robots. Lilienthal and Duckett [5] have developed algorithms for generating odor concentration grid maps using a chemosensor array onboard a mobile robot. Russell [6] has investigated trail marking and navigation strategies for mobile robots. Ishida et al. [7] have developed an "odor compass" for navigating odor plumes towards their source.

Biologically-inspired odor processing models for chemosensor arrays have also received much attention in recent years. Ratton et al. [8] have employed the olfactory model of Ambros-Ingerson et al. [9], which simulates the closed-loop interactions between the olfactory bulb and higher cortical areas, to classify data from micro-hotplate metal oxide sensors. White et al. [10, 11] have employed a spiking neuron model of the peripheral olfactory system to process signals from fiber-optic sensor array. Pearce et al. [12] have investigated the issue of concentration hyperacuity by means of massive convergence of ORNs onto GL. Otto et al. have employed the KIII model of Freeman et al. [13] to process data from chemical sensors [14]. Our prior work [15, 16] has investigated the issue of habituation for processing odor mixtures with chemical sensor arrays.

In this paper we adapt three primitives from the early olfactory pathway: convergence of olfactory receptor neurons (ORNs) onto glomeruli (GL), center on-off surround inter-glomerular connections, and slow adaptation of mitral (M) cells in response to sustained stimuli. These computational primitives are validated on experimental data from an array of temperature-modulated metal-oxide semiconductor (MOS) chemoresistors. Our results are consistent with recent findings from neurobiology, and show that the model is able to solve the problems of concentration-invariant odor detection and contrast enhancement through spatio-temporal patterning.

II. MODEL

Fig. 1 illustrates the key building of our neuromorphic model: (i) ORN-GL chemotopic convergence, (ii) center on-off surround lateral inhibition and (iii) slow adaptation. A detailed description of the model follows.

This research was supported by NSF CAREER award 9984426/0229598

0-7803-8463-6/04/$20.00 ©2004 IEEE

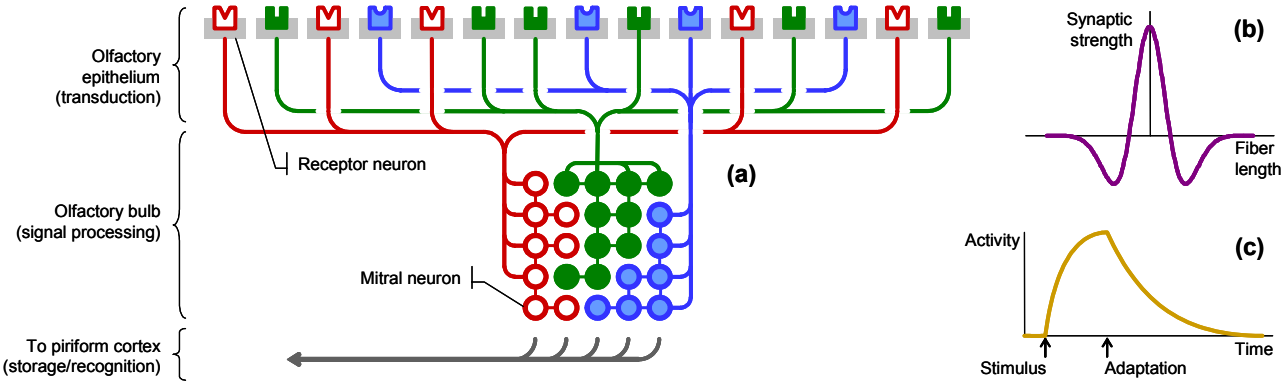

Fig. 1. (a) Structure of the proposed model. Receptor neurons in the olfactory epithelium converge onto the olfactory bulb in a chemotopic manner, forming the first organized representation of a stimulus: an olfactory image. (b) Center on – off surround lateral interactions enhances the contrast of the initial spatial pattern. (c) Finally, local habituation adds a temporal dimension to the spatial representation, leading to a pseudo-periodic attractor.

A. Population coding

A fundamental difference between machine and biological olfaction is the dimensionality of the input space. The biological olfactory system employs a large population of ORNs (100 million neurons in the human olfactory epithelium, replicated from 1,000 primary receptor types), whereas its artificial analogue uses very few sensors. With a few exceptions [12], e-noses normally do not contain more than 32 sensors, primarily for practical reason (i.e., cost) but also due to theoretical constraints (i.e., molecular determinants of odor quality are yet unknown).

To simulate a large population of cross-selective sensors, we employ a sensor excitation technique known as temperature modulation. The response of a MOS sensor to a volatile compound is partly dependent on its operating temperature, which is controlled by applying a voltage to a built-in heater. Therefore, varying the heater voltage during exposure to a volatile, and capturing the sensor response at multiple temperatures, typically yields more information than that provided by the sensor response at the constant set-point temperature specified by the manufacturer [17]. In other words, the response of a sensor at a particular temperature can be treated as a separate "pseudo-sensor," and therefore used to simulate a large population of ORNs. (refer to Fig. 2(a)).

B. Chemotopic mapping

The projection from the olfactory epithelium onto the olfactory bulb is organized such that ORNs expressing same receptor gene converge to one or a few GL [18], globular structures of neuropil on which ORNs synapse mitral cells. This convergence transforms the initial combinatorial code into an organized spatial pattern (i.e. an olfactory image), which decouples odor identity from intensity [19]. In addition, massive convergence improves the signal to noise ratio by integrating signals from multiple receptor neurons [20, 12].

In [19] we have proposed a theoretical model of chemotopic convergence based on three principles: (i) ORNs with similar affinities project onto neighboring GL, (ii) GLs in the olfactory bulb are spatially arranged as a two-dimensional surface, and (iii) neighboring GL tend to respond to similar odors [21, 22]. Therefore, a natural choice to model the ORN-GL convergence is the self-organizing map (SOM) of Kohonen [23]. In this article we apply our previous model as follows:

- A large population of ORNs is obtained through temperature modulation: one pseudo-sensor equals one ORN, and
- ORN affinity is approximated by the response of the pseudo-sensor to a set of C volatile compounds.

Therefore, in what follows we will refer to pseudo-sensors as ORNs, and the SOM nodes to which the pseudo-sensors converge as GL. The SOM is presented with a population of ORNs, each represented by a vector in C-dimensional affinity space, and trained to model this probability distribution (see Fig. 2(b)). Once the SOM is trained, each ORN is then assigned to the closest GL in affinity space, thereby forming a convergence map from which the response of each GL can be computed as

$$G_j^A = \sum_{i=1}^{N} W_{ij} R_i^A \qquad (1)$$

where R_i^A is the response of ORN_i to odorant A, N is the number of ORNs, and W_{ij}=1 if ORN_i converges to GL_j and zero otherwise.

This convergence model works well when the different sensors are reasonably uncorrelated, since then the projection of ORNs across the SOM lattice approximates a uniform distribution, i.e., maximum entropy [24]. Unfortunately, the population of pseudo-sensors created by temperature modulation is extremely collinear. As a result, a few GL tend to receive the majority of ORNs, which capture the "common-mode" response of the sensor, overshadowing the most discriminatory information in the temperature-modulated response. To avoid this issue, the activity of each GL is normalized by the number of ORNs that converge to it:

$$G_j^A = \frac{\sum_{i=1}^{N} W_{ij} R_i^A}{\sum_{i=1}^{N} W_{ij}} \tag{2}$$

Note that this solution is not driven by biological plausibility but largely by the limitations of our sensors.

C. Center on-off surround lateral interaction

The initial glomerular image is further transformed in the olfactory bulb (OB) by means of two distinct lateral inhibitory circuits. The first of these circuits, which occurs between mitral and inhibitory periglomerular (PG) cells, has been suggested to perform some form of "volume control" to broaden the dynamic range of concentrations at which an odorant can be identified [25]. The second circuit occurs through interaction between mitral and inhibitory granule (G) cells at the output of the OB. Two roles have been suggested for this granule-mediated circuit: (i) sharpening of the molecular tuning range of individual mitral cells [26], and (ii) global redistribution of activity such that the bulb-wide representation of an odorant, rather than the individual tuning ranges, becomes specific and concise over time [20].

More recently, both lateral circuits have been found to be center on-off surround inhibitory [27] (Fig. 1(b)), an organization reminiscent of the classical receptive fields mediated by ganglion cells in the retina [28]. This form of lateral inhibition performs a winner-take-all (WTA) competition, where strongly excited units suppress weakly excited ones. In the retina, center-surround leads to edge detection and discrimination of objects by size. In the context of olfaction, these circuits have been suggested to perform pattern normalization, noise reduction and contrast enhancement of the spatial patterns in the OB [27].

We model this center on-off surround circuit with the classical additive model from neurodynamics [29, p. 676], whose general form is:

$$\frac{dv_j^A(t)}{dt} = -\frac{v_j^A(t)}{\tau_j} + \sum_{\substack{k=1 \\ k \neq j}}^{M} L_{kj}\varphi\left(v_k^A(t)\right) + I_j^A \tag{3}$$

where v_j is the activity of mitral neuron j, τ_j is the time constant that captures the dynamics of the neuron, L_{kj} is the synaptic weight between neurons k and j, M is the number of neurons, and I_j is the external input defined by (2), properly scaled to balance the contribution of receptor and lateral inputs $\left(I_j^A = 10G_j^A\right)$. Our model assumes a one-to-one mapping between GL and M neurons: although GL are known to project to several M neurons, the computational function of this divergence mapping is largely unknown. The non-linear activation $\varphi(\cdot)$ is the logistic function defined by:

$$\varphi\left(v_j\right) = \frac{1}{1 + \exp(-a_1 \cdot (v_j - a_2))} \tag{4}$$

where the constants a_1 and a_2 are set to 0.0589 and 49.9900, respectively, to maximize the dynamic range of v_j. For simplicity, all mitral neurons are assumed to have the same time constant τ=10ms. Integration of (3) with Euler's method leads to a difference equation:

$$\begin{aligned} v_j^A(t+\Delta t) &\cong v_j^A(t) + \Delta t \frac{dv_j^A(t)}{dt} = \\ &\left(1 - \frac{\Delta t}{\tau}\right) v_j^A(t) + \sum_{\substack{k=1 \\ k \neq j}}^{M} L_{kj}\varphi\left(v_k^A(t)\right)\Delta t + I_j^A \Delta t \end{aligned} \tag{5}$$

To model center on-off surround, each neuron makes excitatory synapses to nearby units and inhibitory synapses with distant units as follows:

$$L_{kj} = \begin{cases} U(0,1) & d(k,j) < \frac{1}{5}\sqrt{M} \\ U(-1,0) & \frac{1}{5}\sqrt{M} \le d(k,j) < \frac{2}{5}\sqrt{M} \end{cases} \tag{6}$$

where $U(a,b)$ is a uniform distribution between a and b, d is the distance between units measured as a Euclidean distance within the lattice ($d = \sqrt{(r_k - r_j)^2 + (c_k - c_j)^2}$; r and c being the row and column coordinates of a neuron in the lattice). Self-connections are disabled ($L_{jj}=0$). Thus, the output of a given mitral neuron is determined by the combined effect of external inputs from ORNs, center on – off surround interactions with collateral neurons, as well as by its own dynamics.

D. Temporal patterning through adaptation

In addition to the spatial activity across glomerular (or mitral) units, the olfactory system uses time as an additional coding dimension [30]. Friedrich and Laurent [31] have shown that the spatial activity in the bulb becomes specific and concise over the course of a stimulus, thus further reducing the overlap between odor representations.

To model the temporal aspects of olfactory coding we introduce a habituation term $h(t)$, which models the slow adaptation of a neuron in the presence of a sustained stimulus [32]:

$$\begin{aligned} &\frac{dv_j^A(t)}{dt} = -\frac{v_j^A(t)}{\tau} + \sum_{\substack{k=1 \\ k \neq j}}^{M} L_{kj}\varphi\left(v_k^A(t)\right) + I_j^A - h_j(t) \\ &\frac{dh_j(t)}{dt} = -\frac{1}{\tau_H} h_j(t) + \delta(t - t_H); \\ &t_H = \left\{t; \left[v_j(t) - V_H = 0\right] \wedge \left[dv_j(t)/dt > 0\right]\right\} \end{aligned} \tag{7}$$

where τ_H is the habituation time constant (τ_H = 50 ms), $\delta(\cdot)$ is the Dirac delta function, and t_H defines those times at which habituation is triggered, which occurs when a neuron reaches a threshold V_H as a result of sustained stimulation. In our model, $\delta(0) = 100$ and $V_H=0.95$. Using Euler's integration (Δt=1ms), and combining with (5) yields:

$$\begin{aligned} v_j^A(t+1) &\cong \left(1 - \frac{1}{\tau}\right) v_j^A(t) + \sum_{\substack{k=1 \\ k \neq j}}^{M} L_{kj}\varphi\left(v_k^A(t)\right) + I_j^A - h_j(t) \\ h_j(t+1) &\cong \left(1 - \frac{1}{\tau_H}\right) h_j(t) + \delta(t - t_H) \end{aligned} \tag{8}$$

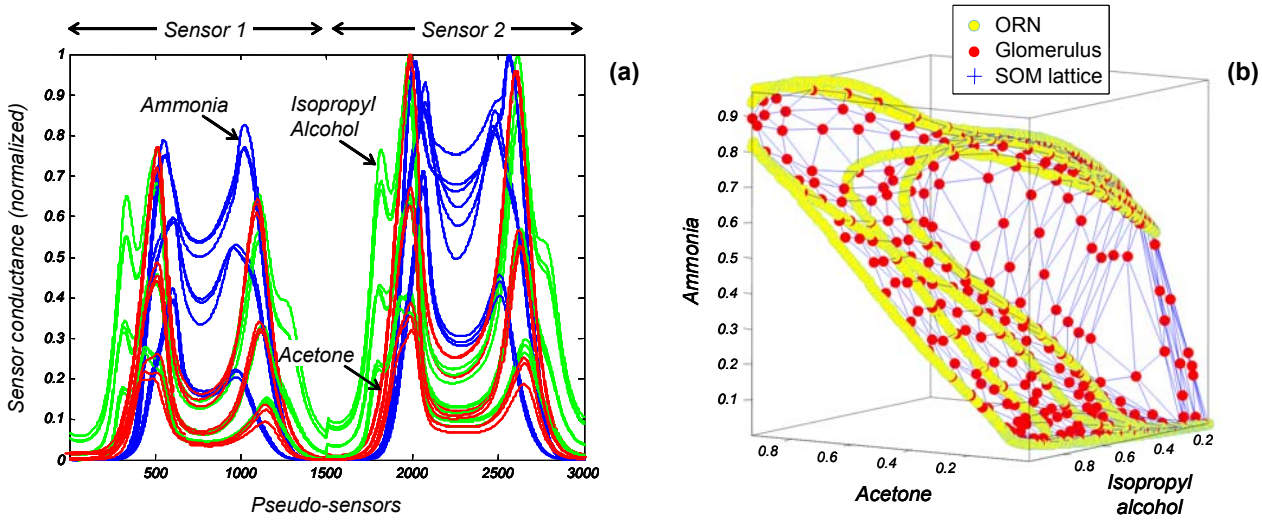

Fig. 2. (a) Temperature modulated response of two MOS sensors (concatenated) to acetone (odor A), isopropyl alcohol (odor B) and ammonia (odor C) at three concentrations. Three replicates per analyte and concentration are shown in the figure to illustrate the repeatability of the patterns. (b) Distribution of glomerular SOM nodes and pseudo-sensor repertoire in affinity space (3,000 ORNs, 20×20 lattice).

This model is functionally similar to the delayed self-inhibition model proposed in [33] for odor segmentation. Adaptation causes M cells that are most active to dominate at first, and slowly habituate. This allows slightly less active cells, which were suppressed earlier, to become more active. Hence the more prominent features of an odor are contributed first to the temporal patterning, followed by the more subtle features. This causes spatial odor patterns, which may have very similar initial activity, to evolve and become unique over time. If allowed to evolve over the course of multiple adaptation periods, the network activity becomes a pseudo-periodic dynamic attractor.

III. Results

To validate the model, we have used a database of temperature-modulated sensor patterns for three analytes acetone (A), isopropyl alcohol (B) and ammonia (C), at three different concentrations. Two Figaro MOS sensors (TGS 2600, TGS 2620) [34] were temperature modulated using a sinusoidal heater voltage (0-7 V; 2.5min period; 10Hz sampling frequency). The response of the two sensors to the three analytes at the three concentration levels is shown in Fig. 2(a). Each point in the temperature cycle is considered as a separate pseudo-sensor, thus resulting in a population of N=3,000 pseudo-sensors. This population projects onto a GL layer with M=400 nodes arranged as a 20×20 lattice. The SOM arranges itself to model the affinity space, as shown in Fig. 2(b).

A. Spatial patterning

The chemotopic projection of pseudo-sensor responses onto the GL layer generates a gross spatial pattern with a high degree of overlap across patterns, as shown in Fig. 3 (top row). Odors A and B, which produce similar responses on the MOS sensors, also lead to very similar GL maps prior to processing with the center on – off surround network. Fig. 3 (middle row) shows the resulting GL maps following stabilization of the center-surround lateral interactions as modeled in (5) (no habituation). Odor A leads to heavy activation of regions 1 and 3 (spatial code: 13). Odor B produces similar activation in regions 1 and 3, but also high activation in region 4 (spatial code: 134). This unique region 4 corresponds to pseudo-sensors in the smaller peak that occurs for odor B alone (refer to Fig. 2(a)). Odor C produces heavy activation of regions 1, 2 and 5 (spatial code: 125). It is important to note that the location of these activation regions is concentration-invariant, but their amplitude and spread increases with concentration, in consistency with recent finding in neurobiology [35].

The center-surround lateral connections have the effect of correlating nearby units and decorrelating distant ones. The width of the receptive fields plays a significant role in this process. Widespread lateral connectivity leads to sparser representations, since a single GL region can dominate the competition and suppress activity elsewhere in the lattice. Small receptive fields, on the other hand, allow for finer discrimination of similar odor features, e.g., as is required to disambiguate regions 2 and 3 in Fig. 3.

B. Temporal patterning

The results presented in the previous subsection were based on the sole effect of convergence and center-surround inhibition. Temporal patterning can be induced if mitral cells are allowed to habituate above a threshold activity. Fig. 4(a) shows the average activity over time in each of the five coding regions when the habituation model in equation (8) is used. Activity during the first 50ms is driven by the center-surround interactions; subsequent oscillations are due to habituation. As a result of the habituation dynamics, the spatial code is transformed into a spatio-temporal pattern, where information is jointly encoded in the amplitude, phase and frequency of the signals. Frequency modulation can be clearly observed in the second region of Fig. 4(a): odors A, B and C present 3, 2 and 5 peaks, respectively, during the first 1000ms. Fig. 4(b) shows the global activity across the network projected onto the first three principal components. Odor trajectories originate fairly close to one another but move away and settle into odor-specific attractors.

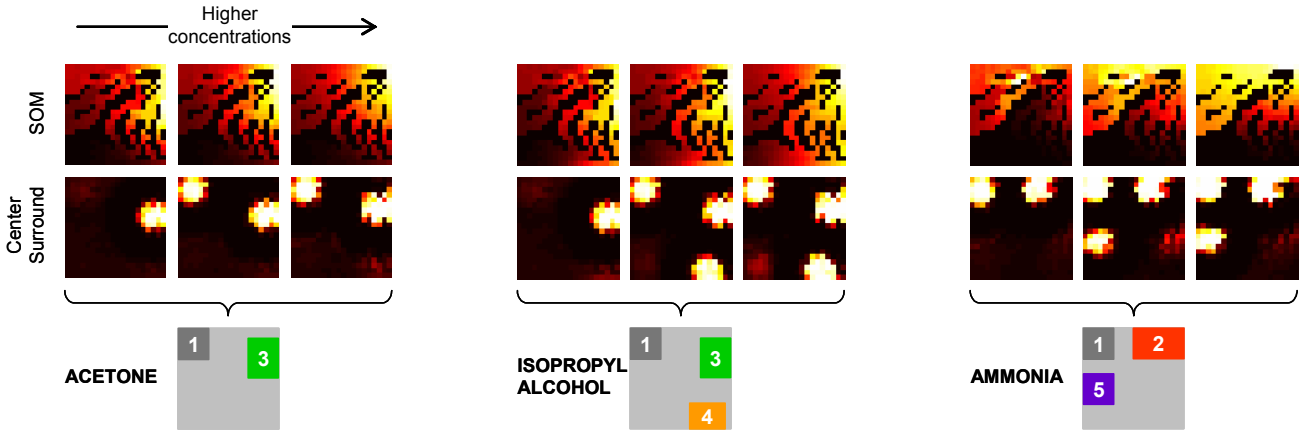

Fig. 3. Initial spatial maps generated by the chemotopic convergence (top row), and after stabilization of the center on-off surround lateral interactions (middle row). No habituation was used to produce these results. The bottom row shows the five sparse coding regions that emerge as a result of the lateral interactions.

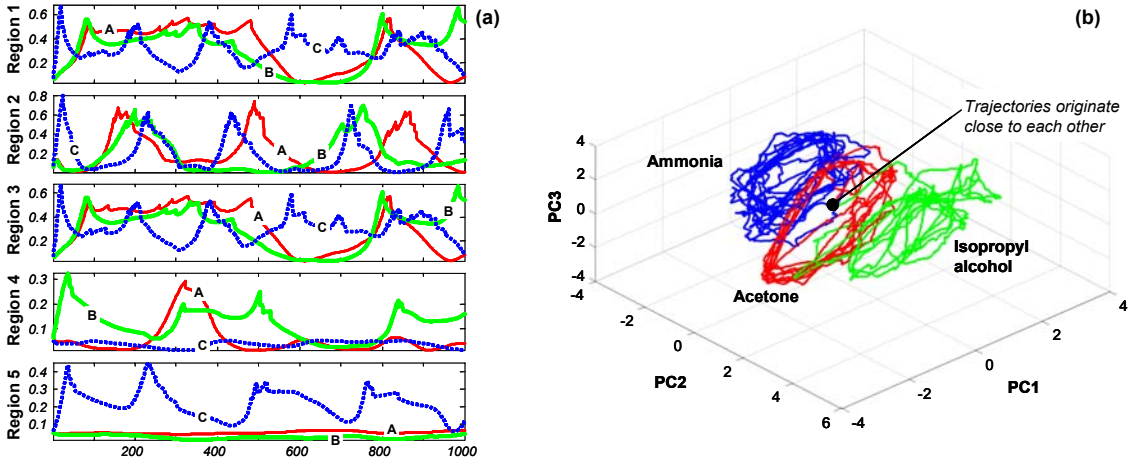

Fig. 4. Temporal coding as a result of habituation. (a) Temporal evolution of the average activity in each of the five coding areas shown in Fig. 3 for the highest concentration of the three analytes. Odor information is encoded in the amplitude, phase and frequency of these signals; frequency modulation can be clearly observed in region 2. (b) Projection of the global activity on the 400 neurons (20×20 lattice) onto the first three principal components. Trajectories initiate close to each other, but eventually move to distinct attractor wings in state space.

C. *Stability analysis*

The stability of the dynamic networks in (5) and (8) was analyzed by computing the Lyapunov exponents of their trajectories in state space. Given a fiduciary and a test orbit with close initial conditions, the largest Lyapunov λ_1 can be computed as follows [36]:

$$\lambda_1 = \frac{1}{t_F - t_0} \sum_{n=1}^{F} \log_2 \frac{d'(t_n)}{d(t_{n-1})} \qquad (9)$$

where *d(t)* is the distance between the fiducial and a test orbit at time t, and *d'(t)* is the distance between them at the end of a predefined time step ($t_n - t_{n-1}$).

In our case, the orbits consist of M-dimensional trajectories, each dimension corresponding to the activity of a given mitral cell with respect to time. The largest Lyapunov exponent for the recurrent network without habituation (5) was found to be negative. This indicates that, for the particular inputs in our experimental dataset, the system converges to a fixed point (i.e., is asymptotically stable). The largest Lyapunov exponent of the recurrent network with habituation (8) was found to be close to zero but positive which, given the results in Fig. 4(b), suggests that the attractors are limit cycles or chaotic.

IV. Summary and Conclusions

We have presented a neuromorphic model for processing chemosensor array signals based on three mechanisms found in the olfactory pathway: chemotopic convergence of ORNs onto GL, center-surround lateral inhibitory in the olfactory bulb, and temporal patterning through habituation of mitral projection cells.

First, a large population of pseudo-sensors is obtained by modulating the operating temperature of a metal-oxide sensor array. The distribution of pseudo-sensors in chemical affinity space is then captured with a Kohonen

self-organizing map. As a result, sensors become clustered according to their selectivity, and a spatial pattern emerges across the lattice.

Based on recent results from neurobiology, a recurrent network with center on-off surround lateral connections is used to process the initial olfactory image in the SOM. This network is able to significantly reduce the overlap between the spatial patterns, and produce a sparser representation on a few selected mitral cells.

Finally, habituation of mitral cells as a result of sustained stimuli allows the model to induce a temporal patterning of the activity in the bulb that further increases the discrimination between odors.

The proposed model presents a biologically-plausible solution for the problem of concentration–invariant discrimination of odors. The next stage in this research is to extend the model to the problems of mixture segmentation and figure-background separation.

REFERENCES

[1] B. Webb, "What does robotics offer animal behavior?" Animal Behavior, vol. 60, pp. 545-558, 2000.

[2] L. Marques, U. Nunes and A. T. de Almeida, "Olfaction-based robot navigation," Thin Solid Films, vol. 418, pp. 51-58, 2002.

[3] F. W. Grasso, T. R. Consi, D. C. Mountain and J. Atema, "Biomimetic robot lobster performs chemo-orientation in turbulence using a pair of spatially separated sensors: Progress and challenges," Journal of Robotics and Autonomous Systems, vol. 30, pp. 115-131, 2000.

[4] A. T. Hayes, A. Martinoli and R. M. Goodman, "Distributed odor source localization," IEEE Sensors Journal, vol. 2, no.3, pp. 260- 271, 2002.

[5] A. Lilienthal and T. Duckett, "Creating Gas Concentration Gridmaps with a Mobile Robot," in Proceedings of the 2003 IEEE/RSJ International Conference on Intelligent Robots and Systems (IROS 2003).

[6] R. A. Russell, Odor detection by mobile robots, World Scientific, Singapore, 1999.

[7] H. Ishida, A. Kobayashi, T. Nakamoto and T. Moriizumi, "Three-dimensional odor compass," IEEE Transactions on Robotics and Automation, vol. 15, no.2, pp. 251-257, 1999.

[8] L. Ratton, T. Kunt, T. McAvoy, T. Fuja, R. Cavicchi, and S. Semancik, "A comparative study of signal processing techniques for clustering microsensor data (a first step towards an artificial nose)," Sensors and Actuators, vol.B41, no. 1-3, pp. 105-120, 1997.

[9] J. Ambros-Ingerson, R. Granger and G. Lynch, "Simulation of paleocortex performs hierarchical clustering," Science, vol. 247. pp. 1344-1348, 1990.

[10] J. White, T. A. Dickinson, D. R. Walt and J. S. Kauer, "An olfactory neural network for vapor recognition in an artificial nose," Biol. Cybern., vol. 78, pp. 245-251, 1998.

[11] J. White and J. S. Kauer, "Odor recognition in an artificial nose by spatio-temporal processing using an olfactory neuronal network," Neurocomputing 26-27, pp. 919-924, 1999.

[12] T. C. Pearce, P.F.M.J. Verschure, J. White and J.S. Kauer, "Robust Stimulus Encoding in Olfactory Processing: Hyperacuity and Efficient Signal Transmission," in S. Wermter, J. Austin and D. Willshaw, Eds. Emergent Neural Computation Architectures Based on Neuroscience, Springer-Verlag, 2001, pp. 461-479.

[13] H. J. Chang, W. J. Freeman and B. C. Burke, "Biologically modeled noise stabilizing neurodynamics for pattern recognition," International Journal of Bifurcation and Chaos, vol. 8., no. 2, pp. 321-345, 1998.

[14] M. Otto, S. Quarder, U. Claußnitzer and J. Lerchner, "A nonlinear dynamic system for recognizing chemicals based on chemical sensors and optical spectra," in Proc. World Multiconference on systemics, Cybernetics and Informatics (SCI-2000), vol. X, pp. 413-418, 2000.

[15] R. Gutierrez-Osuna and A. Gutierrez-Galvez,, "Habituation in the KIII olfactory model with chemical sensor arrays," IEEE Transactions on Neural Networks, vol. 16. pp. 649-656, 2003.

[16] R. Gutierrez-Osuna and N. U. Powar, "Odor Mixtures and Chemosensory Adaptation in Gas Sensor Arrays," International Journal on Artificial Intelligence Tools, vol. 12, no.1, pp.1-16, 2003.

[17] A. P. Lee and B. J. Reedy, "Temperature modulation in semiconductor gas sensing," Sensors and Actuators, vol. B60, pp. 35-42, 1999.

[18] R. Vassar, S. K. Chao, R. Sitcheran, J. M. Nunez, L. B. Vosshall and R. Axel, "Topographic Organization of Sensory Projections to the Olfactory Bulb," Cell, vol. 79, pp. 981-991, 1994.

[19] R. Gutierrez-Osuna, "A Self-organizing Model of Chemotopic Convergence for Olfactory Coding," in Proceedings of the 2nd Joint EMBS-BMES Conference, Houston, TX, pp. 23-26, 2002.

[20] G., Laurent, "A Systems Perspective on Early Olfactory Coding," Science, vol. 286. no. 22. pp. 723-728, 1999.

[21] M. Meister, T. Bonhoeffer, "Tuning and topography in an odor map on the rat olfactory bulb," Journal of Neuroscience, vol. 21. no.4. pp. 1351-1360, 2001.

[22] B. A. Johnson and M. Leon, "Modular representation of odorants in the glomerular layer of the rat olfactory bulb and the effects of stimulus concentration," Journal of Comparative Neurology, vol. 422, pp. 496-509, 2000.

[23] T. Kohonen, "Self-organized formation of topologically correct feature maps," Biol. Cybern., vol. 43. pp. 59-69, 1982.

[24] J. Laaksonen, M. Koskela, and E. Oja, "Probability interpretation of distributions on SOM surfaces," in Proceedings of Workshop on Self-Organizing Maps (WSOM'03), Hibikino, Kitakyushu, Japan, 2003, pp. 77-82.

[25] W. Freeman, "Olfactory system: odorant detection and classification," in D. Amit and G.Parisi (Eds.), Building blocks for Intelligent Systems: Brain components as Elements of Intelligent Function, vol. III, part 2, Academic Press, New York, 1999.

[26] K. Mori, H. Nagao, and Y. Yoshihara, "The Olfactory Bulb: Coding and Processing of Odor molecule information," Science, vol. 286, pp.711-715, 1999.

[27] J. L. Aungst, P. M. Heyward, A. C. Puche, S. V. Karnup, A. Hayar, G. Szabo and M. T. Shipley, "Center-surround inhibition among olfactory bulb glomeruli," Nature, vol. 26, pp. 623- 629, 2003.

[28] S. W. Kuffler, "Discharge patterns and functional organization of mammalian retina," J. Neurophysiol, vol. 16, pp. 37-68, 1953.

[29] S. Haykin, Neural Networks: A Comprehensive Foundation, 2nd Ed., Englewood Cliffs, NJ: Prentice-Hall, 1999, pp.676.

[30] G. Laurent, "Olfactory network dynamics and the coding of multidimensional signals," Nature Reviews Neuroscience, vol. 3, pp. 884-895, 2002.

[31] R. Friedrich and G. Laurent, "Dynamic optimization of odor representation by slow temporal patterning of mitral cell activity," Science, vol. 291, pp. 889-894, 2001.

[32] D. L. Wang, "Habituation," in M.A. Arbib (Ed.), The Handbook of Brain Theory and Neural Networks, MIT Press, pp. 441-444, 1995.

[33] D. L. Wang, J. Buhmann, and C. von der Malsburg, "Pattern segmentation in associative memory," Neural Computation, vol. 2, pp. 94-106, 1990.

[34] Figaro 1996, Figaro Engineering, Inc., Osaka, Japan.

[35] R.W. Friedrich and S.I. Korsching, "Combinatorial and chemotopic odorant coding in the zebrafish olfactory bulb visualized by optical imaging," Neuron, vol. 18, pp. 737-752, 1997.

[36] A. Wolf, J. B. Swift, H. L. Swinney, and J. A. Vastano, "Determining lyapunov exponents from a time series," Physica D, vol. 16, pp. 285-317, 1985.